Chemical Science

ROYAL SOCIETY OF CHEMISTRY

EDGE ARTICLE

View Article Online
View Journal | View Issue

Cite this: *Chem. Sci.*, 2025, **16**, 8807

All publication charges for this article have been paid for by the Royal Society of Chemistry

Received 3rd March 2025
Accepted 7th April 2025

DOI: 10.1039/d5sc01685a

rsc.li/chemical-science

Redox mediated dimerisation of a *cyclo*-As_8 complex†

Christoph Riesinger and Manfred Scheer *

Reduction as well as oxidation of the *cyclo*-As_8 complex [{Cp″Ta}$_2$(μ,$\eta^{2:2:2:2:1:1}$-As_8)] (A, Cp″ = 1,3-^{t}Bu$_2$C$_5$H$_3$) are demonstrated to afford controlled dimerisation to unprecedented As_{16} species. The dication [{Cp″Ta}$_4$(μ$_4$,$\eta^{2:2:2:2:2:2:2:1:1:1:1}$-$As_{16}$)]$^{2+}$ slowly disproportionates in solution, yielding the largest polyarsenide species in a molecular complex known to date.

Compared to its lighter homologs in group 15, nitrogen and phosphorus, the chemistry of arsenic is highly underdeveloped.[1,2] Although arsenic is crucial in applications such as semiconductor manufacturing (*e.g.* GaAs),[3–5] arsines, for example, are far less utilised in fields like catalysis, when compared to ubiquitous phosphines.[6] Of course, this is most notably due to the higher toxicity associated with arsenic compounds. Nevertheless, arsenic species often hold chemical advantages over their lighter homologs rendering their exploration of significant fundamental value.[2] For example, transition metal stabilised polyarsenide (As_n) ligands[7] can be employed in the preparation of organometallic coordination compounds.[8–10] This often results in distinct structural motifs which drastically differ from those of their lighter polyphosphorus (P_n) analogues.[11,12] However, these As_n ligand complexes are far less accessible due to the limited availability of starting materials (*e.g.* yellow arsenic, As_4).[2] Furthermore, their reactivity remains underexplored compared to the lighter P_n species, which have received considerable interest in the light of sustainable transformation of white phosphorus P_4.[13–15] Thus, the functionalisation and transformation of As_n ligand complexes offer potential routes towards novel As_n scaffolds.[16,17] Most notably, the redox chemistry of those complexes may serve as a promising starting point for the preparation of unprecedented molecular polyarsenides. However, oxidation and reduction of end-deck As_n complexes have been demonstrated to result in more or less uncontrolled fragmentations,[18,19] which can be attributed to the low As–As bond energy (146 kJ mol^{-1}) compared to *e. g.* P–P bonds (220 kJ mol^{-1}).[20] A prominent example for such unselective reactivity is found in the reduction of [Cp*Fe(η^5-As_5)] (Cp* = C_5Me_5, Fig. 1a),[21] which is in stark contrast to the redox chemistry of its lighter congener [Cp*Fe(η^5-P_5)].[22] The associated difficulties in sample purification hamper the utilisation of the polyarsenide products in synthetic applications. Furthermore, the hardly accessible ^{75}As (I = 3/2) NMR spectroscopy fails as a tool to analyse reaction mixtures when compared to the widely used ^{31}P NMR spectroscopy. On the other hand, the redox chemistry of As_n triple decker complexes and cluster compounds generally resulted in only minor structural changes and did not afford new As_n scaffolds.[23,24] Thus, the As_2 ligands in [{Cp‴Co}$_2$(μ,$\eta^{2:2}$-As_2)$_2$] (Cp‴ = 1,2,4-^{t}Bu$_3$C$_5$H$_2$) underwent only intramolecular bond formation upon oxidation as well as reduction (Fig. 1b).[25]

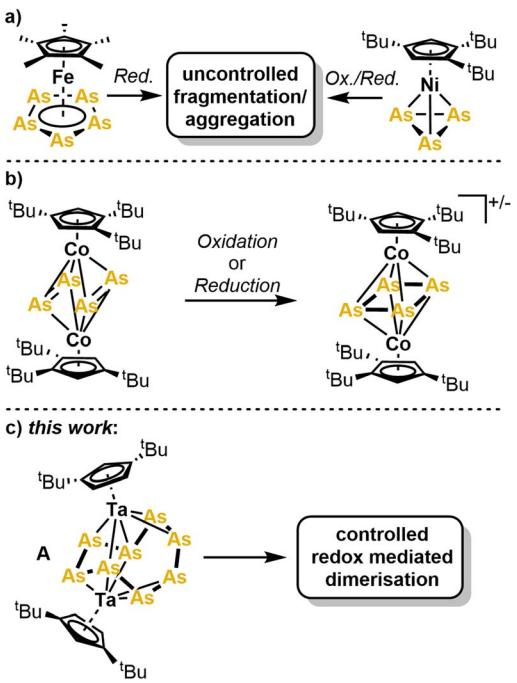

Fig. 1 Previously reported redox chemistry of As_n ligand complexes (a and b) and unprecedented dimerisation of [{Cp″Ta}$_2$(μ,$\eta^{2:2:2:2:1:1}$-As_8)] (A) to As_{16} species (c).

Institute of Inorganic Chemistry, University of Regensburg, Universit, ä, tsstr 31, 93053 Regensburg, Germany. E-mail: manfred.scheer@chemie.uni-regensburg.de

† Electronic supplementary information (ESI) available. CCDC 2421973–2421975. For ESI and crystallographic data in CIF or other electronic format see DOI: https://doi.org/10.1039/d5sc01685a

Similarly, oxidation of a hexaarsa-benzene ligand in [{Cp*Mo}$_2$(μ,$\eta^{6:6}$-As$_6$)] leads to a bisallylic distortion and formation of the respective radical cation.[26] Only when the bimetallic [{CpMo(CO)$_2$}$_2$(μ,$\eta^{2:2}$-As$_2$)] was oxidised a controlled intermolecular As–As bond formation to an As$_4$ chain was observed.[27]

Expanding this reactivity to complexes with larger As$_n$ ligands could enable the synthesis of yet unprecedented molecular polyarsenides but has not yet been realised. The *cyclo*-As$_8$ ligand complex [{Cp″Ta}$_2$(μ,$\eta^{2:2:2:2:1:1}$-As$_8$)] (**A**, Cp″ = 1,3-^{t}Bu$_2$C$_5$H$_2$)[28] appears to be a promising candidate for studying its redox behaviour. Herein we present the controlled and selective redox mediated dimerisation of this complex (Fig. 1c). In view of the recent preparation and study of the coordination behaviour as well as redox chemistry of the *cyclo*-P$_8$ complex [{Cp‴Ta}$_2$(μ,$\eta^{2:2:2:2:1:1}$-P$_8$)] (**B**),[29] starting with the *cyclo*-As$_8$ analogue **A** could deliver unprecedented molecular polyarsenides.

Initially, the redox properties of **A** were assessed electrochemically by cyclic voltammetry (−2.7 V to 1.3 V, 30 mg in 10 mL of *o*-DFB with 1000 mg [^{n}Bu$_4$N][PF$_6$] as supporting electrolyte; see ESI for further details, Fig. S1†). This revealed two synthetically accessible, but irreversible, redox events at −1441 mV and 294 mV (*vs.* FcH/FcH$^+$), respectively. Thus, the strong reducing agent KC$_8$ and salts of the strongly oxidising [Thia]$^+$ (Thia = thianthrene, C$_{12}$H$_8$S$_2$) radical cation were chosen to investigate the reactivity of **A** experimentally. Exposing **A** to one equivalent of KC$_8$ in THF at −80 °C leads to an immediate colour change from light brown to dark brownish black. As the product was expected to be highly sensitive, [2.2.2]-cryptand was added directly into the reaction mixture. After warming to room temperature, filtration and layering with *n*-hexane the product [K@crypt]$_2$[{Cp‴Ta}$_4$-(μ_4,$\eta^{2:2:2:2:2:2:2:2:1:1:1:1}$-As$_{16}$)] (**1**) was isolated as nearly black crystalline blocks in yields of 90% (Fig. 2). The dianion in **1** features an unprecedented catena-As$_{16}$ ligand arising from the dimerisation of **A**. Similarly, oxidation of **A** with one equivalent of [Thia][TEF] (Thia = thianthrene, [TEF]$^-$ = [Al{OC(CF$_3$)$_3$}$_4$]$^-$) in *o*-DFB (1,2-difluorobenzene) at −30 °C leads to a dimerisation and [{Cp‴Ta}$_4$(μ_4,$\eta^{2:2:2:2:2:2:2:2:1:1:1:1}$-As$_{16}$)][TEF]$_2$ (**2**) was isolated as a dark brown powder in 80% yield after precipitation from the reaction solution with *n*-pentane (Fig. 2). **2** can be stored as a solid indefinitely but slowly disproportionates, even at 4 °C, when kept in solution for several days. Notably, **1** and **2** display only the second and third example of controlled redox-mediated dimerisation of a polyarsenic ligand complex.[27] The solid state structure of **1** reveals two mostly intact As$_8$ ligands of **A** being dimerised *via* the former As$_4$ atoms (in **A**, Fig. 2). However, the As1–As8 distance of 3.083(1) Å agrees with this bond being cleaved (the corresponding As4–As4′ bond in **A** is 2.537(2) Å long).[28] In contrast, the newly formed As1–As1′ bond (2.441(1) Å) is in the range of a single bond (2.42 Å).[30] The remaining As–As bonds (2.403(1)–2.458(1) Å) are similar in length implying no localised multiple bond character for any of them. Furthermore, the Ta1–Ta2 distance of 3.354(1) Å is identical to that found in **A** (3.353(1) Å) and confirms that a weak metal–metal interaction (*vide infra*) is present in **1**. On the other hand, layering a concentrated solution of **2** in *o*-DFB with *n*-pentane and storage at 4 °C affords dark rod-shaped crystals of this compound within 1–2 weeks. **2** features two intact *cyclo*-As$_8$

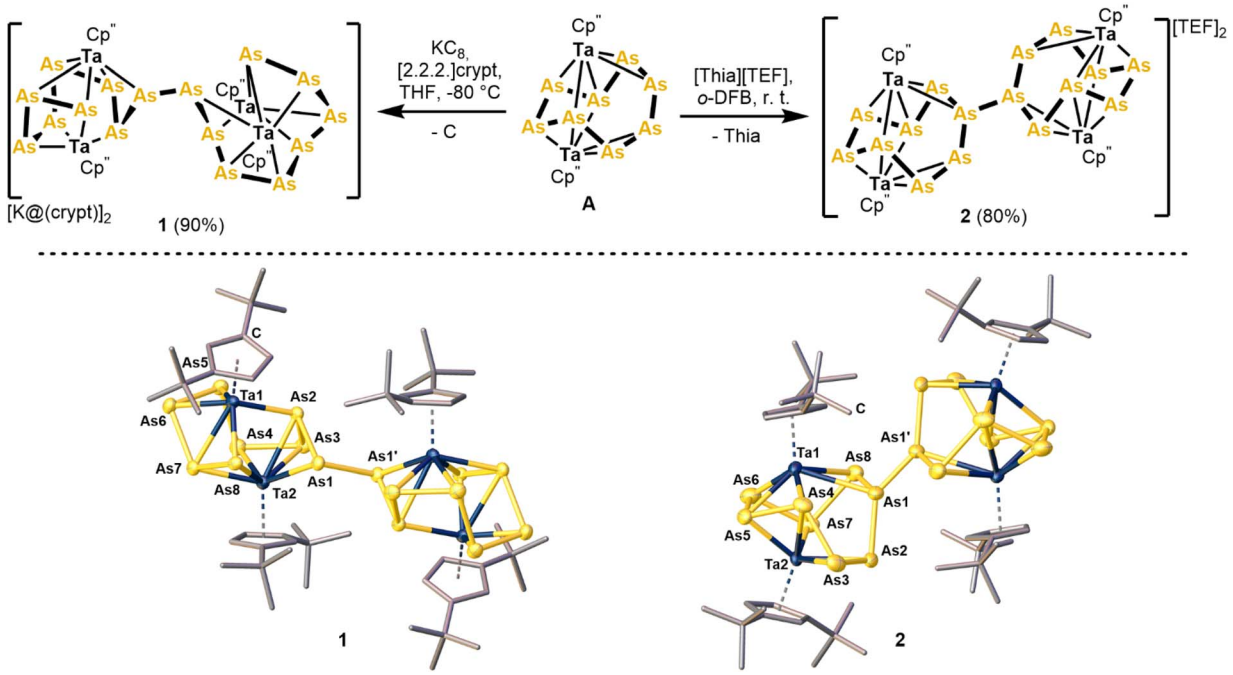

Fig. 2 Synthesis of **1** and **2** *via* reduction and oxidation of **A**, respectively (top) and molecular structures of the dianion **1** and the dication **2** in the solid state (bottom); anisotropic displacement parameters are drawn at the 50% probability level and H atoms as well as counter-ions are omitted for clarity.

groups being linked by a central As1–As1′ bond. While the formal bond length of the latter (2.120(3) Å) is shorter than an expected single bond (2.42 Å),[30] this can be attributed to packing effects but especially to a complex disorder within the cationic core of this compound (see ESI† and computational results, *vide infra*). In contrast to **1**, the As5–As6 bond (2.621(2) Å) is only slightly elongated when compared to the respective As4–As4′ bond in **A** (2.537(2) Å). The other As–As bonds are similar in length (2.370(2) – 2.493(2) Å) and in the range of single bonds.[30] Notably, the Ta1–Ta2 distance in **2** (3.253(3) Å) is about 0.1 Å shorter compared to **A**.[28] Both compounds, **1** and **2**, are isostructural to their lighter P analogues arising from reduction and oxidation of **B**, respectively.[29] Nevertheless, the catena-As_{16} ligand in **1** is unprecedented and the dication in **2** represents the largest dicationic polyarsenide in general. The integrity of both compounds **1** and **2** was additionally verified by elemental analysis, ^{1}H, and ^{19}F NMR spectroscopy (see ESI†). Additionally, the ESI(+) mass spectrum of **2** reveals the molecular ion peak of its dication, further corroborating these results. Both compounds can be stored as solids under inert conditions for several months without showing signs of degradation. However, when **2** is kept in CH_2Cl_2 or *o*-DFB solution for more than a week it partly decomposes in a complex disproportionation reaction, affording two novel polyarsenide complexes **3** and **4**. This disproportionation could not be circumvented by lowering the temperature, changing the solvent or the utilisation of other counter anions. On the one hand, the arsenic depleted complex $[\{Cp''Ta\}_2(\mu,\eta^{1:1:1:1:1:1}\text{-}As_6)][TEF]$ (**3**, Fig. 3) bears a central *cyclo*-As_6 ligand bridging two Ta centers. It shows As–As bond lengths (2.380(3) – 2.545(3) Å) in the range of single bonds, with only the As1–As6 distance (2.728(2) Å) being significantly elongated.[30] On the other hand, this disproportionation leads to the formation of the arsenic rich $[\{Cp''Ta\}_6(\mu_6,\eta^{2:2:2:2:2:2:2:2:2:2:2:2:1:1:1:1:1:1:1}\text{-}As_{25})][TEF]_3$ (**4**) representing the largest molecular polyarsenide known so far (see ESI† and Fig. 3). In **4** formally three units of **A** are linked by one central As atom, thus leading to the formation of the As_{25} ligand. The central As1/As1′–As9 bond lengths (2.533(2)–2.553(2) Å) in **4** are in the range of elongated single bonds, which may be a result of steric hindrance around the central As9 atom. The remaining As–As bonds (2.164(2) – 2.611(2) Å) are similar to those in **A**.[28] Unfortunately, both **3** and **4** cannot be separated, neither from residual **2** nor from each other, as all three compounds co-crystallise, which hinders their isolation and spectroscopic characterisation. However, the integrity of the triple-decker cation in **3** and even the trication in **4** could be confirmed by ESI(+) mass spectrometry (see ESI†). To get deeper insight into the molecular and electronic structure of **1** and **2** computational investigations were carried out on the ωB97X-D4/def2-TZVP level of theory (Fig. 4). In general, the molecular structures of both compounds are well reproduced in these computations. Furthermore, the As1–As1′ bond in the computed structure of **2** (2.503 Å) is closer to the expected As–As single bond length compared to the crystallographic data (2.120(3) Å). This corroborates the assumption that the observed bond length in the solid state is a result of packing effects, as well as a complex disorder (*vide supra*). Furthermore, NBO analysis consolidates the bonding between the monomeric subunits of **1** and **2** to occur *via* localised As–As single bonds with Wiberg bond indices close to unity (**1** : 0.92, **2** : 0.84). Thus, potential multiple bonding, as suggested by the short As1–As1′ bond in the X-ray structure of **2**, can be ruled out.

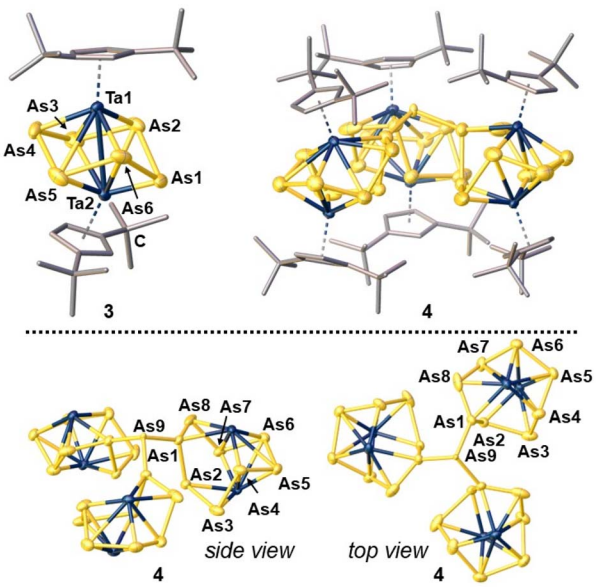

Fig. 3 Molecular structures of **3** and **4** in the solid state (top) as well as a side-on and top-down representation of the heavy atom core in **4** (bottom); anisotropic displacement parameters are drawn at the 50% probability level and H atoms (and C atoms at the bottom) as well as anions are omitted for clarity.

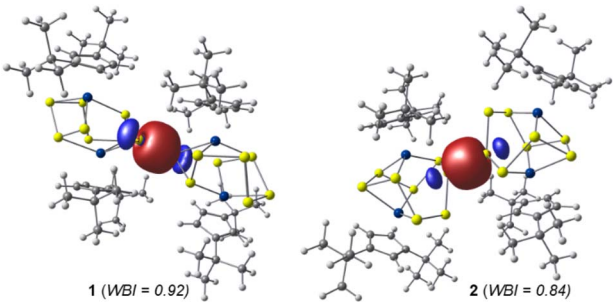

Fig. 4 Computed molecular structures of the dianion $[\mathbf{1}]^{2-}$ (left) and the dication $[\mathbf{2}]^{2+}$ (right) with the NBOs of the corresponding As1–As1′ bonds; cut-off at 0.4 a. u.

Conclusions

In conclusion, contrasting known polyarsenic ligand complexes, the redox mediated dimerisation of the *cyclo*-As_8 ligand complex **A** proceeds selectively and results in two unprecedented polyarsenide scaffolds. The dianion $[K@crypt]_2[\{Cp''Ta\}_4(\mu_4,\eta^{2:2:2:2:2:2:2:2:1:1:1:1}\text{-}As_{16})]$ (**1**) features a novel As_{16} chain, while $[\{Cp''Ta\}_4(\mu_4,\eta^{2:2:2:2:2:2:2:2:1:1:1:1}\text{-}As_{16})][TEF]_2$ (**2**) represents the largest dicationic polyarsenide known to date. The latter is shown to be unstable towards disproportionation, when kept in solution for prolonged times. This

results in the formation of the *cyclo*-As_6 triple decker complex $[\{Cp''Ta\}_2(\mu,\eta^{1:1:1:1:1:1}\text{-}As_6)][TEF]$ (**3**) as well as the arsenic rich trication $[\{Cp''Ta\}_6(\mu_6,\eta^{2:2:2:2:2:2:2:2:2:2:2:2:1:1:1:1:1:1}\text{-}As_{25})][TEF]_3$ (**4**), which marks the largest molecular polyarsenide ligand isolated so far. Additional computational data elaborates the bonding situation in the dimeric complexes **1** and **2**.

Data availability

The authors confirm that the data supporting the findings of this study are available within the article and its ESI.†

Author contributions

The conceptualisation (together with MS), experimental work and writing of the manuscript of this work were achieved by CR. CR accomplished the solution and refinement of X-ray structural data and performed the DFT calculations. The entire work was supervised, guided, and revised by MS, who also acquired funding for the project. The final manuscript was reviewed and edited by CR and MS.

Conflicts of interest

There are no conflicts to declare.

Acknowledgements

This work was supported by the Deutsche Forschungsgemeinschaft (DFG) within the project Sche384/36-2. C. R. is grateful to the Studienstiftung des Deutschen Volkes for a PhD fellowship. The authors thank Benjamin Falge for assistance with conducting the cyclic voltammetry studies. Additional references are cited within the ESI.† [27,28,31–51]

Notes and references

1 A. F. Holleman, E. Wiberg and N. Wiberg, *"Lehrbuch der Anorganischen Chemie"*, Walter de Gruyter, Berlin (DE), 2007, pp. 822–860.
2 M. Seidl, G. Balázs and M. Scheer, *Chem. Rev.*, 2019, **119**, 8406.
3 R. L. Wells and W. L. Gladfelter, *J. Cluster Sci.*, 1997, **8**, 217.
4 S. Schulz in. *"Advances in Organometallic Chemistry"*, Elsevier, 2003, pp. 225–317.
5 B. Neumüller and E. Iravani, *Coord. Chem. Rev.*, 2004, **248**, 817.
6 J. H. Downing and M. B. Smith in. *"Comprehensive Coordination Chemistry II"*, Elsevier, 2003, pp. 253–296.
7 O. J. Scherer, *Angew Chem. Int. Ed. Engl.*, 1990, **29**, 1104.
8 M. Fleischmann, S. Welsch, H. Krauss, M. Schmidt, M. Bodensteiner, E. V. Peresypkina, M. Sierka, C. Gröger and M. Scheer, *Chem.–Eur. J.*, 2014, **20**, 3759.
9 M. E. Moussa, J. Schiller, E. Peresypkina, M. Seidl, G. Balázs, P. Shelyganov and M. Scheer, *Chem.–Eur. J.*, 2020, **26**, 14315.
10 M. E. Moussa, M. Fleischmann, G. Balázs, A. V. Virovets, E. Peresypkina, P. A. Shelyganov, M. Seidl, S. Reichl and M. Scheer, *Chem.–Eur. J.*, 2021, **27**, 9742.
11 M. Fleischmann, J. S. Jones, F. P. Gabbaï and M. Scheer, *Chem. Sci.*, 2015, **6**, 132.
12 M. Fleischmann, L. Dütsch, M. E. Moussa, A. Schindler, G. Balázs, C. Lescop and M. Scheer, *Chem. Commun.*, 2015, **51**, 2893.
13 B. M. Cossairt, N. A. Piro and C. C. Cummins, *Chem. Rev.*, 2010, **110**, 4164.
14 M. Caporali, L. Gonsalvi, A. Rossin and M. Peruzzini, *Chem. Rev.*, 2010, **110**, 4178.
15 C. M. Hoidn, D. J. Scott and R. Wolf, *Chem. - Eur. J.*, 2021, **27**, 1886.
16 S. Reichl, C. Riesinger and M. Scheer, *Angew. Chem., Int. Ed.*, 2023, **62**, e202307696.
17 S. Reichl, C. Riesinger, R. Yadav, A. Y. Timoshkin, P. W. Roesky and M. Scheer, *Angew. Chem., Int. Ed.*, 2024, **63**, e202316117.
18 M. Schmidt, A. E. Seitz, M. Eckhardt, G. Balázs, E. V. Peresypkina, A. V. Virovets, F. Riedlberger, M. Bodensteiner, E. M. Zolnhofer, K. Meyer and M. Scheer, *J. Am. Chem. Soc.*, 2017, **139**, 13981.
19 C. Riesinger, L. Zimmermann and M. Scheer, *Organometallics*, 2023, **42**, 2065.
20 N. K. Kildahl, *J. Chem. Educ.*, 1995, **72**, 423.
21 M. Schmidt, D. Konieczny, E. V. Peresypkina, A. V. Virovets, G. Balázs, M. Bodensteiner, F. Riedlberger, H. Krauss and M. Scheer, *Angew. Chem., Int. Ed.*, 2017, **56**, 7307.
22 M. V. Butovskiy, G. Balázs, M. Bodensteiner, E. V. Peresypkina, A. V. Virovets, J. Sutter and M. Scheer, *Angew. Chem., Int. Ed.*, 2013, **52**, 2972.
23 M. Piesch, S. Reichl, C. Riesinger, M. Seidl, G. Balazs and M. Scheer, *Chem.–Eur. J.*, 2021, **27**, 9129.
24 C. Riesinger, L. Dütsch and M. Scheer, *Z. Anorg. Allg. Chem.*, 2022, **648**, e202200102.
25 M. Piesch, C. Graßl and M. Scheer, *Angew. Chem., Int. Ed.*, 2020, **59**, 7154.
26 M. Fleischmann, F. Dielmann, G. Balázs and M. Scheer, *Chem.–Eur. J.*, 2016, **22**, 15248.
27 L. Dütsch, M. Fleischmann, S. Welsch, G. Balázs, W. Kremer and M. Scheer, *Angew. Chem., Int. Ed.*, 2018, **57**, 3256.
28 K. Mast, J. Meiers, O. J. Scherer and G. Wolmershäuser, *Z. Anorg. Allg. Chem.*, 1999, **625**, 70.
29 C. Riesinger, F. Dielmann, R. Szlosek, A. V. Virovets and M. Scheer, *Angew. Chem., Int. Ed.*, 2023, **62**, e202218828.
30 P. Pyykkö, *J. Phys. Chem. A*, 2015, **119**, 2326.
31 **https://omics.pnl.gov/software/molecular-weight-calculator**, (22.01.2025).
32 J.-M. Lalancette, G. Rollin and P. Dumas, *Can. J. Chem.*, 1972, **50**, 3058.
33 Agilent, *CrysAlis PRO*, Agilent Technologies Ltd, Yarnton, Oxfordshire, England, 2014.
34 O. V. Dolomanov, L. J. Bourhis, R. J. Gildea, J. A. K. Howard and H. Puschmann, *J. Appl. Crystallogr.*, 2009, **42**, 339.
35 G. M. Sheldrick, *Acta Crystallogr., Sect. A*, 2015, **71**, 3.

36 G. M. Sheldrick, *Acta Crystallogr., Sect. C:Struct. Chem.*, 2015, **71**, 3.
37 G. M. Sheldrick, *Acta Crystallogr., Sect. A*, 2008, **64**, 112.
38 F. Neese, *Wiley Interdiscip. Rev.: Comput. Mol. Sci.*, 2012, **2**, 73.
39 F. Neese, *Wiley Interdiscip. Rev.: Comput. Mol. Sci.*, 2018, **8**, e1327.
40 F. Neese, F. Wennmohs, U. Becker and C. Riplinger, *J. Chem. Phys.*, 2020, **152**, 224108.
41 F. Neese, *Wiley Interdiscip. Rev.: Comput. Mol. Sci.*, 2022, **12**, e1606.
42 F. Neese, *J. Comput. Chem.*, 2023, **44**, 381.
43 A. D. Becke, *Phys. Rev. A:At., Mol., Opt. Phys.*, 1988, **38**, 3098.
44 F. Weigend and R. Ahlrichs, *Phys. Chem. Chem. Phys.*, 2005, **7**, 3297.
45 J. Tomasi, B. Mennucci and R. Cammi, *Chem. Rev.*, 2005, **105**, 2999.
46 E. D. Glendening, C. R. Landis and F. Weinhold, *J. Comput. Chem.*, 2019, **40**, 2234.
47 J.-D. Chai and M. Head-Gordon, *Phys. Chem. Chem. Phys.*, 2008, **10**, 6615.
48 J.-D. Chai and M. Head-Gordon, *J. Chem. Phys.*, 2008, **128**, 84106.
49 Y.-S. Lin, G.-D. Li, S.-P. Mao and J. D. Chai, *J. Chem. Theory Comput.*, 2013, **9**, 263.
50 E. Caldeweyher, S. Ehlert, A. Hansen, H. Neugebauer, S. Spicher, C. Bannwarth and S. Grimme, *J. Chem. Phys.*, 2019, **150**, 154122.
51 *Chemcraft - graphical software for visualization of quantum chemistry computations*, **https://www.chemcraftprog.com**, (22.01.2025).